Basic Limits for LTE-Advanced Radio and HetNet Optimization in the Outdoor-to-indoor Scenario

Fernando J. Velez[1,2] and Sofia Sousa[1]
[1]Instituto de Telecomunicações – DEM
Universidade da Beira Interior, Faculdade de Engenharia
6201-001 Covilhã, Portugal
fjv@ubi.pt, sofia.sousa@lx.it.pt

Albena Mihovska and Ramjee Prasad[2]
Center for TeleInfrastruktur (CTIF)
Department of Electronic Systems, Aalborg University
9220 Aalborg, Denmark
albena@es.aau.dk, prasad@es.aau.dk

***Abstract*—The unplanned deployment of small cells is leading to high levels of intra- and inter-tier interference. An insight on how to manage the interference is vital to reach a significant capacity improvement through ultra-dense networks. This paper considers heterogeneous networks with carrier aggregation, where the macro cells operate at 800 MHz to provide coverage and the small cells operate at 2.6 GHz to provide throughput enhancement at hotspots, including an outdoor-to-indoor scenario. We analyze in detail the values of the carrier-to-noise-plus-interference ratio (CNIR) from/at the user equipment (UE) for bandwidths of 10 and 20 MHz. A rapid decay is observed in the throughput for the small cells at a distance < 300m. Broader bandwidths allow for doubling the capacity only for $R>d_{BP}/r_{cc}$. For R>250m, the capacity is similar for reuse pattern, K=3 and 7, showing no advantages for higher K. A clear decrease of the supported throughput is verified for the highest coverage distances in non-line-of-sight propagation conditions. Besides, one concludes that outdoor-to-indoor coverage corresponds to slightly worst coverage with less interference.**

Keywords— System capacity; LTE-A; Outdoor-to-indoor; CNIR; ITU-R propagation model; Radio and HetNet optimization

I. INTRODUCTION

Today, both the usage of mobile services and applications and the pace, at which this use grows, is accelerating. According to [1], in 2013 mobile data traffic was nearly 18 times the size of the entire global Internet in 2000. The deployment of macro cells overlaid with several small cells (SCs), also known as heterogeneous networks (HetNets) has been proposed for increasing the network capacity and coverage, to eliminate coverage holes and to provide coverage in indoor and outdoor areas. SCs can be pico cells, relays and femtocells [2]. Carrier aggregation (CA) has been proposed as a solution to meet the exponential growth of the network traffic, as well as the fragmented spectrum attribution to operators nowadays. The core of this work is to define the basic limits on a scenario where the macro cells (operating at 800 MHz, and providing full coverage) are overlaid by SCs (operating at 2.6 GHz, and providing higher throughputs). The paper provides a comprehensive study on the variation of the DL carrier-to-noise-plus-interference ratio (CNIR) from/at the user equipment (UE) with different system parameters, which is critical in the context of LTE-Advanced optimization. The variation of CNIR with the coverage and reuse distances is analyzed for different values of the channel quality indicator (CQI) and the respective modulation and coding scheme (MCS), at the macro and pico cellular layers of an LTE-A HetNet. The focus is on the Outdoor-to-Indoor (O-t-I) pico cell deployment model (e.g., outdoor SC antennas on top of buildings "illuminating" to the inside of large buildings that have large percentage of glass surfaces).

Table I shows the mapping established with the MCS index and the vertical asymptote obtained for each MCS, for the pico scenario for bandwidths of 10 MHz and 20 MHz. An outdoor SC scenario and the O-t-I propagation SC scenario are considered. In a previously published work [3], a similar Table was derived for the macro cellular layer.

The power and gains assumed in the considered LTE scenario are shown in Table II for the 800-MHz/2.6-GHz operating frequencies.

TABLE I. MINIMUM CNIR, MODULATION AND SPECTRAL EFFICIENCY VERSUS MCS, FOR LTE, AND VALUES FOR THE VERTICAL ASYMPTOTE FOR DL

Mod. index	Vertical asymptote							
	f = 2.6 GHz, pico, Outdoor				*f = 2.6 GHz, pico, O-to-I*			
	10 MHz	10 MHz NLoS	20 MHz	20 MHz NLoS	10 MHz	10 MHz NLoS	20 MHz	20 MHz NLoS
1	4.666	1.009	3.924	0.836	1.106	0.209	0.930	0.173
2	4.401	0.947	3.701	0.784	1.044	0.196	0.878	0.162
3	4.151	0.889	3.491	0.736	0.984	0.184	0.828	0.152
4	3.865	0.822	3.250	0.681	0.917	0.170	0.771	0.141
5	3.599	0.761	3.026	0.630	0.853	0.157	0.718	0.130
6	3.342	0.702	2.810	0.581	0.792	0.145	0.666	0.120
7	3.138	0.655	2.639	0.542	0.744	0.136	0.626	0.112
8	2.906	0.603	2.444	0.499	0.689	0.125	0.580	0.103
9	2.722	0.561	2.289	0.465	0.646	0.116	0.543	0.096
10	2.512	0.514	2.112	0.425	0.596	0.106	0.501	0.088
11	2.317	0.471	1.948	0.390	0.549	0.097	0.462	0.081
12	2.242	0.454	1.886	0.376	0.532	0.094	0.447	0.078
13	2.170	0.438	1.825	0.363	0.515	0.091	0.433	0.075
14	2.011	0.403	1.691	0.334	0.477	0.083	0.401	0.069
15	1.863	0.371	1.567	0.307	0.442	0.077	0.371	0.064
16	1.713	0.339	1.440	0.280	0.406	0.070	0.342	0.058
17	1.575	0.309	1.324	0.256	0.373	0.064	0.314	0.053
18	1.531	0.300	1.288	0.248	0.363	0.062	0.305	0.051
19	1.489	0.291	1.252	0.241	0.353	0.060	0.297	0.050
20	1.350	0.261	1.135	0.216	0.320	0.054	0.269	0.045
21	1.223	0.235	1.028	0.194	0.290	0.049	0.244	0.040
22	1.132	0.216	0.952	0.178	0.268	0.045	0.226	0.037
23	1.048	0.198	0.881	0.164	0.248	0.041	0.209	0.034
24	0.985	0.185	0.828	0.153	0.234	0.038	0.196	0.032
25	0.926	0.173	0.778	0.143	0.220	0.036	0.185	0.030
26	0.801	0.148	0.674	0.122	0.190	0.031	0.160	0.025
27	0.693	0.126	0.583	0.105	0.164	0.026	0.138	0.022
28	0.582	0.104	0.489	0.086	0.138	0.022	0.116	0.018
29	0.488	0.086	0.410	0.071	0.116	0.018	0.097	0.015

978-1-5090-1925-0/16/$31.00 ©2016 IEEE

TABLE II. POWER, GAIN AND NOISE PARAMETERS

Parameters	f [GHz]	P_t[dBW]	G_t[dBi]	G_r[dBi]	BW[MHz]	N_f [dB]
Macro/Pico	0.8 / 2.6	16 / -7	17	0	10 / 20	5

The rest of the paper is organized as follows. Section II defines the overlaid scenario with macro cells, small cells with O-t-I coverage and CA. Section III builds upon an existing analysis of the pico cellular LTE system capacity considering the assumptions for different levels of MCSs, and gives original analytical results for the equivalent supported throughput as a function of the coverage distance. Finally, Section IV concludes the paper and provides guidelines for future work.

II. CELLULAR RADIO AND HETNET OPTIMIZATION

In HetNets, the cellular radio/network optimization must simultaneously consider the interference and noise in obtaining the maximum coverage distance, which is a critical limitation in the cellular systems dimensioning process. Therefore, cellular optimization has to simultaneously consider carrier-to-noise and carrier-to-interference constraints. This work evaluates a 3GPP Carrier Aggregation (CA) scenario [4]. The authors of [5] have evaluated the DL performance characterized by a macro cell sector overlaid onto four SCs, obtaining a total DL cell throughput of 3.9-fold improvement compared to a conventional macro-cell-only network deployment using two frequency bands. Figure 1 shows a scenario that implements SCs by Remote Radio Heads (RRHs), which are connected to the same baseband processing unit (BBU). The SCs operate in the higher frequency bands for the higher rates, and the MCs operate in a lower band providing full coverage. This scenario [7] allows for a flexible use of the fragmented spectrum in different frequency bands. A frequency of 800 MHz, at the macro base station (eNB) layer provides coverage, while the 2.6-GHz frequency band at a pico-cell layer would improve the throughput at hotspots. Mobility through CA is performed by the macro cells. LoS and NLoS propagation are considered. The pico-cell scenario also considers O-t-I propagation, the choice for which was made because it has been estimated that approximately 80% of data traffic will come from indoor locations [6]. In the absence of a femtocell providing indoor coverage it is crucial to understand the behavior of the pico cells providing throughput to the indoor users. Figure 1 details the scenario of the macro- and pico-cellular environments. The macro cell, has a cell range from 150m to 3000m and provides coverage. The SCs, are overlaying the macro cell, with a cell rage of 25m to 300m to provide throughput.

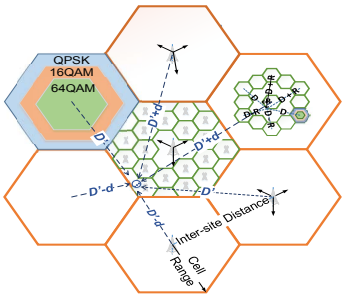

Fig. 1. Coverage and reuse in pico plus macro cellular HetNet, where co-channel interference is represented in the worst-case for the DL.

A. Characterization of the Macro and Pico Scenario

A basic hexagonal layout per macro-cell site is considered. The pico-cell sites consider omnidirectional SC eNBs placed in regular grids and conforming to a hexagonal layout. This work considers the macro and micro/pico cellular scenarios of the ITU-R model [8] for the 800-MHz and 2.6-GHz frequency bands, respectively [9].

The **urban microcellular** (pico-cell) scenario test environment focuses on SCs, high user densities and traffic loads, in city centres and dense urban areas. The channel model is called urban micro (UMi). The key characteristics of this test interference limited environment are high traffic loads, as well as either outdoor or O-t-I coverage. The radio access points are at the level of or below the rooftop. The **urban macrocellular** (macro cell) scenario focuses on large cells and continuous and ubiquitous coverage in urban areas. The channel model is called urban macro (UMa). UEs are located outdoor, at street level and the fixed base stations (eNBs) are clearly above the surrounding building heights. NLoS or obstructed LoS propagation are common cases, since the street level is often reached by a single diffraction over the rooftop.

B. Analytical formulation and channel models for the macro and micro urban scenario

The analytical formulations are a follow up on previously published work [3]. In order to select the appropriate reuse pattern, K, and the appropriate frequency band, radio and network optimization aspects, like the analysis of the cell coverage distance, co-channel reuse factor (ratio between the reuse and coverage distances, r_{cc}), K, and supported throughput are addressed in this work for 29 levels of the LTE MCS.

By considering the dependence of K on r_{cc}, it is straightforward to conclude that, for each value of the propagation exponent, apart from the dependence on the cellular interference geometry, K only depends on the MCS through the corresponding minimum carrier-to-noise ratio.

While the asymptotic reuse factor, r_{cc}, is associated with the upper bound for the system capacity, the maximum coverage distance is associated with the CNIR at the cell boundary when the interference is null. The vertical asymptote, $R_{asymptote}$, from the interference-to-noise ratio, $M(R)$, and $r_{cc}(R)$ represents the interference that can still be tolerated for a given R, in the limit, the maximum coverage distance, for which no extra interference is tolerated.

The following paragraphs define the path loss models considered in the evaluation. These are defined for UMa and are characterized by LoS propagation by a 2 slope model and NLoS propagation. The UMi scenario studies the outdoor scenario and the O-t-I scenario in a hexagonal cell layout. Each of these are characterized for LoS and NLoS propagation. Further, the O-t-I, considers the outdoor path loss model (P_{Lb}) for a hexagonal cell layout with the losses through the wall (P_{Ltw}) and the losses inside the building (P_{Lin}).

The path loss model for the **UMa scenario** is described by Eq. (1)−Eq. (3).

$$P_{L\,UMa\,LoS} = 22\log_{10}(d) + 28 + 20\log_{10}(fc),\ \text{for}\ d < d_{BP} \qquad (1)$$

$P_{L\ UMa\ LoS} = 40\ \log_{10}(d) + 7.8 - 18\ \log_{10}(h'_{BS}),$ for $d > d_{BP}$ (2)
$- \quad 18\ \log_{10}(h'_{UT}) + 2\ \log_{10}(fc).$

$P_{L\ UMa\ NLoS} = 161.04 - 7.1\ \log_{10}(W) + 7.5\ \log_{10}(h) -$
$(24.37 - 3.7(h/h_{BS})\ 2)\ \log_{10}(h_{BS}) +$ (3)
$(43.42 - 3.1\ \log_{10}(h_{BS}))\ (\log_{10}(d) - 3)$
$+ 20\ \log_{10}(f_c) - (3.2\ (\log_{10}(11.75\ h_{UT}))^2 - 4.97)$

Where h_{BS} =25 m and h_{UT}=1.5 m are the heights of the BS and UT, respectively. The variables $h'_{BS[m]}=h_{BS}-1$ and $h'_{UT[m]}= h_{UT} - 1$ are the effective antenna heights at the BS and the UT.

The path loss model for the **UMi scenario** is given by Eq. (4)−Eq. (10).
For the **Outdoor** scenario,

$P_{L\ UMi\ LoS} = 22\ \log_{10}(d) + 28.0 + 20\ \log_{10}(f_c),$ for d< d_{BP} (4)

$P_{L\ UMi\ LoS} = 40\ \log_{10}(d) + 7.8 - 18\ \log_{10}(h'_{BS})$
$-18\ \log_{10}(h'_{UT}) + 2\ \log_{10}(f_c),$ for d> d_{BP} (5)

$P_{L\ UMi\ NLoS} = 36.7\ \log_{10}(d) + 22.7 + 26\ \log_{10}(f_c)$ (6)

For the **O-t-I** scenario,

$P_L = P_{Lb} + P_{Ltw} + P_{Lin},$ (7)

where,

$P_{Lb} = P_{LB}(d_{out}+d_{in}),$ for $10<d_{out}+d_{in}<1000$m (8)

$P_{Ltw} = 20$ (9)

$P_{Lin} = 0.5d_{in},$ for $0<d_{in}<25$m (10)

where h_{BS}=10 m, the street width is 20m, and the average building height is 20m. Variables $h'_{BS[m]}=h_{BS}-1$ and $h'_{UT[m]}= h_{UT} - 1$ also stand. The distance of the break point d_{BP} is calculated by,

$d'_{BP} = 4\ h'_{BS}\ h'_{UT}\ f_c/c$ (11)

where, f_c is the center frequency (Hz), c=3.0 x 10^8m/s is the propagation velocity in free space. Therefore we obtain $d_{BP\ UMa\ LoS}$=128 m and $d_{BP\ UMi\ LoS}$=156 m.

By considering these assumptions, the obtained path loss, in dB, are given by:

$P_{L\ UMa\ LoS}(d) = 22\ \log_{10}(d_{[m]}) + 26.0618,$ for d<128m, (12)

$P_{L\ UMa\ LoS}(d) = 40\ \log_{10}(d_{[m]}) - 11.819,$ for $d\geq$128m. (13)

$P_{L\ UMa\ NLoS}(d) = 39.08639\ \log_{10}(d_{[m]}) + 11.6067$ (14)

$P_{L\ UMi\ LoS}(d) = 22\ \log_{10}(d_{[m]}) + 36.29947,$ for d<156m (15)

$P_{L\ UMi\ LoS}(d) = 40\ \log_{10}(d_{[m]}) - 3.12788,$ for $d\geq$156m (16)

$P_{L\ UMi\ NLoS}(d) = 36.7\ \log_{10}(d_{[m]}) + 33.48,$ (17)

$P_{L\ UMi\ LoS\ O\text{-}t\text{-}I}(d) = 22\ \log_{10}(d_{out}\ [m]) + 61.299,$ for d<156 m (18)

$P_{L\ UMi\ LoS\ O\text{-}t\text{-}I}(d) = 40\ \log_{10}(d_{out}\ [m] + 10)$
$+ 21.87212,$ for d>156m (19)

$P_{L\ UMi\ NLoS\ O\text{-}t\text{-}I}(d) = 36.7\ \log_{10}(d_{out} + d_{in}) + 58.49$ (20)

III. Results

A. Interference-to-noise-ratio

Considering the values for P_t, G_t, G_r, BW and N_f (see, Table II), we obtained the values for the interference-to-noise-ratio, M, in the DL for f = 800 MHz and f = 2.6 GHz. This paper extends the work from [3] by considering now the O-t-I SC scenario. $M(R)$ depends on the CQI value and the MCS associated to it. Table I gives the corresponding values for the vertical asymptote, $R_{asymptote}$, for pico cells operating at 2.6 GHz (LoS/NLoS/ O-t-I), while the asymptotes for the macro cells operating at 800 MHz are addressed in [3]. For the 2.6-GHz case, a relevant decrease in the values for the vertical asymptote (maximum R) occurs as the MCS increases because of the lowest associated $CNIR_{min}$. For O-t-I propagation, a pronounced decrease on the vertical asymptotes is visible for the LoS case, and an even extra reduction is observed for the NLoS case. The decays are explained by the higher losses brought by the walls and inside walls. For Outdoor propagation, NLoS, the propagation exponent is γ =3.67 and the path loss additive constant is higher than before. M is lower, and the asymptotes become visible in the range of Rs ≤ 300m. Besides, an increase in r_{cc} exists. There are limitations in the coverage with the highest MCSs for the shortest Rs. For BW=20 MHz, the vertical asymptotes are slightly shorter compared to BW=10 MHz [3], resulting in worst coverage for short distances.

Figure 2 and Figure 3 show $M(R)$ and $r_{cc}(R)$ for 2.6 GHz ($0\leq R\leq 300$ m), O-t-I scenario, for BW= 10 MHz. In the case of LoS, the propagation exponent is γ=4 and the path loss additive constant is slightly higher than for the outdoor scenario. As the interference becomes lower, M is lower and the asymptotes become now visible in the range of Rs up to 100m. For this case and NLoS, the propagation exponent is γ =3.67 and the path loss additive constant is even higher, resulting in even lower M. For higher bandwidths, the values of M are slightly lower and the vertical asymptotes occur for Rs of only tens of meters. For BW= 20 MHz, although view charts are not presented, slightly shorter coverage distances are achieved.

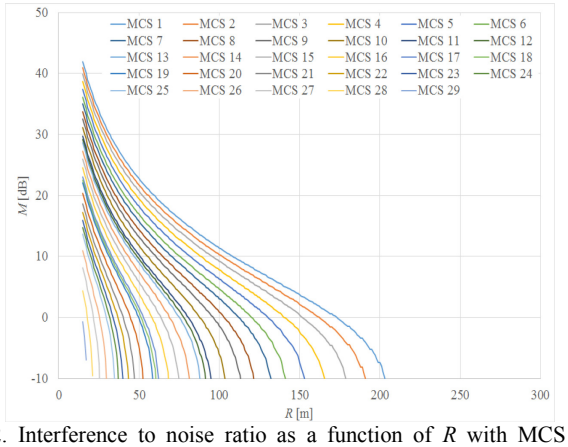

Fig. 2. Interference to noise ratio as a function of R with MCS as a parameter for DL, in the 2.6 GHz band, NLoS, O-t-I, BW=10 MHz.

B. CNIR as a function of r_{cc} with R as parameter

Figure 4 shows the variation of the CNIR with r_{cc}, with R as parameter, for the O-to-I propagation. When the interference power is much higher than noise power, the CNIR is given simply by $C/I \approx r_{cc}^{\gamma}/6$ in linear terms. This occurs in the majority of the cases, as interference, I, is always much higher than noise, N, i.e., M>8-10 dB, except for the cases "2.6 GHz-Outdoor-NLoS-R=300m BW=10 MHz and 20 MHz", "2.6 GHz-O-t-I-LoS-R=300m BW=10 MHz and 20 MHz" and "2.6 GHz-O-t-I-NLoS-R=300m BW=10 MHz and 20 MHz ". Results for CNIR as a function of r_{cc} are discussed in [3] for the Outdoor scenario.

The highest CNIR values are achieved for "O-t-I, NLoS – R= 15m". In the general case, the curves of CNIR with r_{cc} just follow the trend $10 \cdot \gamma \log10(r_{cc}/6)$.

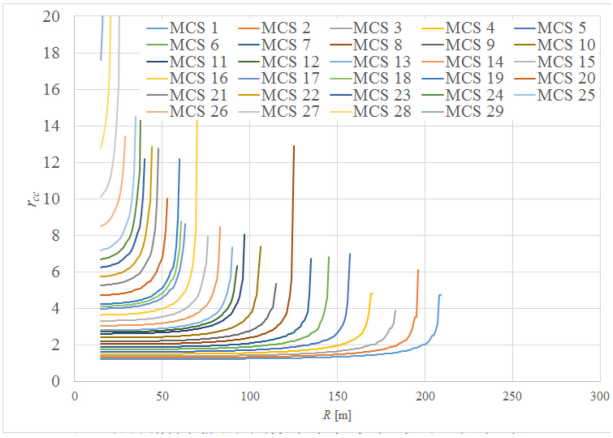

Fig. 3. Co-channel reuse factor as a function of R with MCS as a parameter for DL, in the 2.6 GHz band, NLoS, Outdoor-to-Indoor, BW=10 MHz.

From the propagation models, one can observe that γ varies from 3.67 to 4, except for distances below the breakpoint.

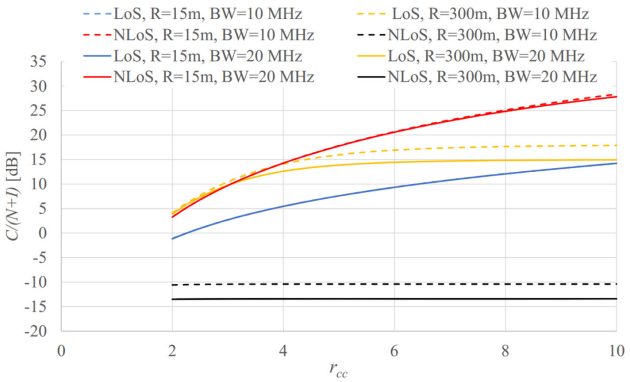

Fig. 4. Variation of the CNIR with r_{cc} for the DL in the 2.6 GHz frequency band, LoS versus NLoS, Outdoor-to-Indoor, BW=10 and 20 MHz.

The exception occurs for the "2.6 GHz-O-t-I-LoS-R=15m" case. In this case, for the purpose of C/I computation, the value of γ is 2.2 (the lowest γ in our analysis). When the system is noise limited (i.e., "2.6 GHz-O-t-I-NLoS-R=300m"), $CNIR(r_{cc})$ follows a trend different from the one represented by $C/I \approx r_{cc}^{\gamma}/6$. Furthermore, if R increases for several hundreds of meters or even some kilometers, the reuse distance ($D=r_{cc} \cdot R$), considerably increases and the interference decreases. The interference becomes, therefore, comparable to the noise and the result will be lower CNIR curves than the upper limit curve.The mapping between these CNIR values and R_b were obtained by considering the correspondence from Table I.

C. Detailed Analysis of the System Capacity

Let us examine the overall impact of several MCSs. Following the formulation in [10] for an implicit function procedure to compute the supported throughput, the LTE system capacity is analyzed for, both, the 800-MHz and the 2.6-GHz cellular layers of a HetNet, based on the ITU-R propagation model [8]. The analysis considers different values of the reuse pattern, e.g., $K = 3$ and $K = 7$. One considers the values for P_t, G_t, G_r, BW and N_f from Table II. To map $CNIR_{min}$ into the supported throughput, we have used the values for $CNIR_{min}$ in [11]. By extrapolating the gathered information, it is possible to map the CNIR into MCS index, Modulation Order Transport Block Size (ITBS) index and TBS.

Figure 5 and Figure 6 analyze the variation of CNIR and throughput (R_b) with the distance d from the cell center to the UE within a cell, where $0 \leq d \leq R$, (see, Figure 2), for the pico-cell, O-t-I scenario, $BW = 10$ MHz and 20 MHz, $K = 7$; 3. In "NLoS", the CNIR and throughput are clearly lower than in "LoS".

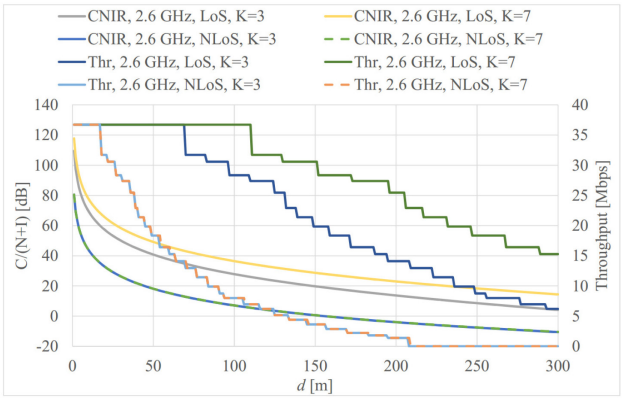

Fig. 5. Comparison of CNIR and R_b between K=7 and 3 for the pico cellular scenario (f=2.6 GHz), BW=10 MHz, and LoS versus NLoS, Outdoor-to-Indoor scenario.

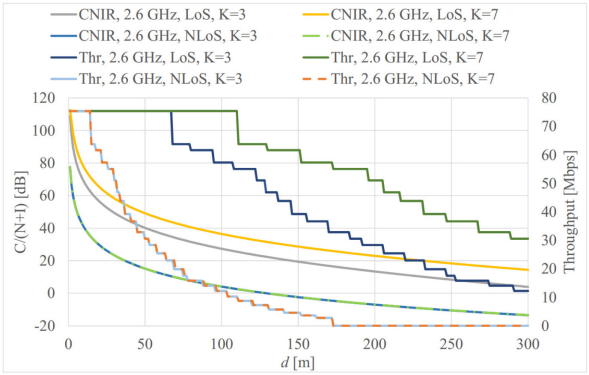

Fig. 6. Comparison of CNIR and R_b between K=7 and 3 for the pico cellular scenario (f=2.6 GHz), BW=20 MHz, and LoS versus NLoS, Outdoor-to-Indoor scenario.

From the mapping of $CNIR_{min}$ and R_b, we clearly observe that the stepwise throughput is close to the maximum near the cell center, and gradually descends for longer distances (as the UE approaches the cell edge). The throughput has a rapid decay, and there is no coverage for the NLoS, R>210m, for BW=10 MHz, and R> 175m, for BW=20 MHz. The comparison of the behavior for BW=10 MHz and BW=20 MHz, shows that the wider the bandwidth, the lower the CNIR. From the results, this evidence is obvious for NLoS propagation but only slightly noticed for the LoS because $N<<I$ and the interference become dominant. Also, we can conclude that for NLoS propagation, indoor SCs should be considered to provide throughput in UE inside buildings. Figure 7 shows the equivalent supported throughput, $R_{b\text{-}sup}$, as a function of R, for an O-t-I scenario and pico-cells with

size up to 300m. $R_{b\text{-}sup}$ is determined through a weighted sum of the PHY throughput in each coverage ring throughout the cell, where the weights are the individual areas of each of the coverage rings. The bandwidth is 10 and 20 MHz. $R_{b\text{-}sup}$ is clearly superior for K=7 than for K=3. At 2.6 GHz (pico cells), as there is no breakpoint in the model for NLoS, the curves have regular behavior. A noticeable behavior is, thus, the decrease in $R_{b\text{-}sup}$ that occurs for the largest Rs, a characteristic from dynamic MCS. As the relevant model for LoS propagation at 2.6 GHz has a breakpoint at 156 m, the behavior of CNIR changes when the values of R reach $R_0 = d_{BP}/r_{cc}$. This means that changes occur for $R_0 = d_{BP}/r_{cc}$=52m for K=3 and R_0=34m for K=7. For $R < d_{BP}/r_{cc}$, the propagation exponents considered in the computation of $C(R)=P_R(R)$ and $I(D, R)$ are the same (γ=2.2). In this range of Rs the supported throughput decreases and then it has a steady behavior (at minimum values). Nevertheless, for $R \geq R_0$, the propagation exponent to compute I is already 4, while the coverage is still computed with γ =2.2. Hence, because of the resulting smaller interference in this range of Rs, a significant increase in the maximum achievable $R_{b\text{-}sup}$ is achieved, followed by a decrease. This analysis gives very useful hints for the optimization of CA [10], [12] between the macro- and pico cellular layer of an LTE-A HetNet with outdoor pico cells as the trade-offs associated with the use of different Ks are highlighted for the LoS/NLoS propagation conditions. The wider the bandwidth is (i.e., 20 MHz, in this case), even if there is a slight decrease in the CNIR, the achieved capacity is circa twice compared to the 10-MHz bandwidth case, for $R > R_0$. For $R >$ 250m, the achieved capacity becomes similar for K=3 and 7, showing no advantages for higher frequency reuse.

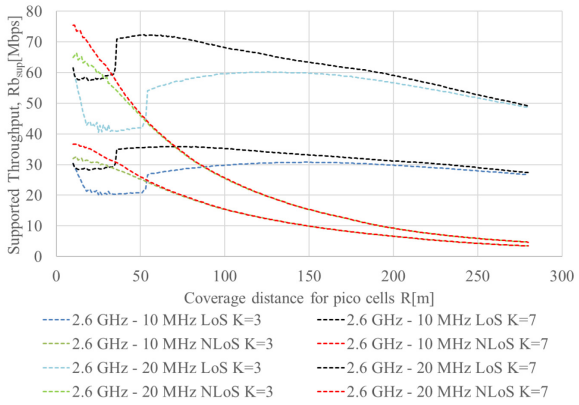

Fig. 7. Comparison of the equivalent supported throughput between K=7 and 3 for the pico cellular scenario and LoS/NLoS, Outdoor-to-Indoor scenario, BW=10 MHz and 20 MHz.

IV. Conclusion

For cellular radio and network optimization purposes, the UL and DL CNIRs from/at the user equipment are very important parameters. This paper provided a detailed analysis of the CNIR variation with the coverage and reuse distances for different LTE-A system parameters, different MSCs in the DL, and for various ITU-R propagation models. We evaluated the possible range for the reuse pattern. By considering the MCS and the reference CNIR requirements recommended by 3GPP, the DL peak bit rates along with the TBS assumed for a single stream and bandwidths of 10 MHz and 20 MHz, an analysis of the physical and supported throughputs was performed. One can learn that a common characteristic of the two frequency bands is the clear decrease of the supported throughput over the coverage distances for NLoS propagation. Besides, for the SC layer, operating at 2.6 GHz, owing to the behavior of the two slope model in LoS (where a breakpoint distance, d_{BP}, exists), a maximum occurs for the system capacity for coverage distances, $R > d_{BP}/r_{cc}$. For the SC layer, due to the increase in the CNIR, the O-t-I model has a slight improvement for shorter Rs, and a decrease in the system capacity (for longer Rs), more pronounced for the NLoS propagation. The results for the O-t-I - NLoS clearly show that for an NLoS UE, in order to guarantee the coverage, a femto cell inside a building should be considered. The obtained results are the basis for the further optimization study of a CA scenario and the focus of planned future work.

Acknowledgment

This work has been partially supported and funded by CREaTION, ECOOP, UID/EEA/50008/2013, EFATraS, SFRH/BSAB/113798/2015, COST CA 15104, and ORCIP.

References

[1] Cisco Visual Networking Index: Global Mobile Data Traffic Forecast Update, 2013-2018, white paper, Feb. 2014.

[2] A. Damnjanovic, J. Montojo, Y. Wei; T. Ji; Tao Luo; M. Vajapeyam; T. Yoo; O. Song; D. Malladi, "A survey on 3GPP heterogeneous networks," *IEEE Wireless Communications*, vol.18, no.3, pp.10,21, June 2011 doi: 10.1109/MWC.2011.5876496

[3] F. J. Velez, S. Sousa, J. Acevedo, D. Robalo, A. Mihovska, R. Prasad, "LTE-Advanced Radio and Network Optimization: Basic Coverage and Interference Constraints", in *Proc. of 15th WPMC*, Hyderabad, India, Dec. 2015.

[4] 3GPP Ts 36.300, V10.8.0 Rel. 10 Evolved Universal Terrestrial Radio Access (E-UTRA) and Evolved Universal Terrestrial Radio Access Network (E-UTRAN); Overall description; Stage 2, July 2012

[5] T., Takiguhi, K., Kiyoshima, Y., Sagae, K. Yagyu, H. Atarashi, S. Abeta, "Performance Evaluation of LTE-Advanced Heterogeneous Network Deployment Using Carrier Aggregation between Macro and Small Cells", *IEICE Trans. Commun.*, vol. E96-B, no. 6, June 2013.

[6] M. Paolini, "Beyond Data Caps – An Analysis of the Uneven Growth in Data Traffic," Senza Fili Consulting, 2011.

[7] M. A. M. Al-Shilby, M. H. Habaebi, J. Chebil, "Carrier aggregation in long term evolution-advanced." in *Proc. of IEEE Control and System Graduate Research Colloquium (ICSGRC) 2012*, 2012. pp. 154-159.

[8] Guidelines for evaluation of radio interface technologies for IMT-Advanced, Report ITU-R M.2135-1, Dec. 2009. (https://www.itu.int/dms_pub/itu-r/opb/rep/R-REP-M.2135-1-2009-PDF-E.pdf).

[9] N. K. Noordin, B. M. Ali, N. Ismail, S.S. Jamuar, "Adaptive techniques in orthogonal frequency division multiplexing in mobile radio environment," *International Journal of Engineering and Technology*, vol. 1, no. 2, 2004.

[10] D. Robalo, *Planning and Dynamic Spectrum Management in Heterogeneous Mobile Networks with QoE Optimization*, Ph.D. thesis, Univesidade da Beira Interior, Covilhã, Portugal, 2014

[11] 3GPP, TS 36.212, V11.3.0. Technical Specification Group Radio Access Network; Evolved Universal Terrestrial Radio Access (E-UTRA); Multiplexing and channel coding, 3GPP Std., June 2013.

[12] J. Acevedo, D. Robalo, F. J. Velez, "Transmitted Power Formulation for the Optimization of Spectrum Aggregation in LTE-A over 800 MHz and 2 GHz Frequency Bands," *Wireless Pers. Comms.*, June 2015.